Research Article

Zhuo Li, Kun Zhang*, Yan Song*, Zhenxue Jiang*, Xiaoxue Liu, Shu Jiang*, Chengzao Jia, Yizhou Huang, Weiwei Liu, Ming Wen, Pengfei Wang, Tianlin Liu, Xuelian Xie, Chang'an Shan, and Xin Wang

Division of shale sequences and prediction of the favorable shale gas intervals: an example of the Lower Cambrian of Yangtze Region in Xiuwu Basin

https://doi.org/10.1515/geo-2019-0015
Received Aug 17, 2018; accepted Mar 13, 2019

Abstract: It is a common method to use sequence stratigraphic theory to identify favourable intervals in hydrocarbon exploration. The Lower Cambrian shale of Well Jiangye-1 in Yangtze Region in Xiuwu Basin was chosen as the research object. The content of excess silicon of siliceous minerals in shale was calculated quantitatively, and the concentration distribution of Al, Fe, Mn showed that the excess silicon is of hydrothermally origin and the shale deposited in an environment with hydrothermal activity. Using U/Th values in the study, combined with lithology and logging data, in order to divide sequences of the Lower Cambrian shale in Yangtze Region in Xiuwu Basin. The result shows that the shale of the Lower Cambrian shale is recognized as 1 2^{nd} sequence (TST-RST, TST = Transgressive systems tract; RST = Regressive systems tract) and then further subdivided into 5 3^{rd} sequences (SQ1-SQ5). During the deposition of SQ2 and SQ3, hydrothermal activity was active, and their excess silicon content was generally above 20%-30%. Rising sea level and active hydrothermal activity were beneficial for the enrichment of siliceous minerals and organic matter. Based on the comparison of the reservoir parameters, it tells that SQ2 and SQ3 have relatively higher content of TOC, higher content of brittle minerals (such as siliceous minerals, carbonate minerals and so on), larger effective porosity and higher content of gas, which make it as the most favourable intervals of the Lower Cambrian in Xiuwu Basin.

Keywords: Hydrothermally activity; Excess silicon; Sequence Stratigraphy; U/Th; Favourable intervals

***Corresponding Author: Kun Zhang:** State Key Laboratory of Petroleum Resources and Prospecting, China University of Petroleum, Beijing 102249, China; Unconventional Natural Gas Institute, China University of Petroleum, Beijing 102249, China; Unconventional Petroleum Collaborative Innovation Center, China University of Petroleum, Beijing 102249, China; Research Institute of Petroleum Exploration and Development, Beijing 100083, China; Energy and Geoscience Institute, University of Utah, Salt Lake City, Utah 84108, United States of America

***Corresponding Author: Yan Song:** State Key Laboratory of Petroleum Resources and Prospecting, China University of Petroleum, Beijing 102249, China; Unconventional Natural Gas Institute, China University of Petroleum, Beijing 102249, China; Research Institute of Petroleum Exploration and Development, Beijing 100083, China; Email: sya@petrochina.com.cn

***Corresponding Author: Zhenxue Jiang:** State Key Laboratory of Petroleum Resources and Prospecting, China University of Petroleum, Beijing 102249, China; Unconventional Natural Gas Institute, China University of Petroleum, Beijing 102249, China; Email: zhenxuejiangedu@126.com

***Corresponding Author: Shu Jiang:** Key Laboratory of Tectonics and Petroleum Resources of Ministry of Education, Faculty of Earth Resources, China University of Geosciences, Wuhan 430074, China; Research Institute of Unconventional Oil & Gas and Renewable Energy, China University of Petroleum (East China), Qingdao 266580, China; Energy and Geoscience Institute, University of Utah, Salt Lake City, Utah 84108, United States of America; Email: jiangsu@cug.edu.cn

Zhuo Li, Xiaoxue Liu, Yizhou Huang, Ming Wen, Tianlin Liu, Xin Wang: State Key Laboratory of Petroleum Resources and Prospecting, China University of Petroleum, Beijing 102249, China; Unconventional Natural Gas Institute, China University of Petroleum, Beijing 102249, China

Chengzao Jia: Research Institute of Petroleum Exploration and Development, Beijing 100083, China

Weiwei Liu: Jiangxi Provincial Natural Gas Company, Ltd., Nanchang 330000, China

Pengfei Wang: Geoscience Documentation Center. China Geological Survey, Beijing 100083, China

Xuelian Xie: Guangzhou Marine Geological survey, Guangzhou 510760, China

Chang'an Shan: School of Earth Sciences and Engineering, Xi'an Shiyou University, Xi'an 710065, China

Zhuo Li, Kun Zhang and Xiaoxue Liu contributed equally to this work

1 Introduction

In recent years, the emergence and development of unconventional hydrocarbon exploration, an advanced understanding of deep water shale depositional systems has occurred. This has resulted in increased production from shale gas resources in North America [1–3]. China also contains significant shale gas resources and commercial development has been implemented in Weiyuan, Changning, Zhaotong, Fushun-Yongchuan, Fuling and Dingshan blocks since 2010 [4–7]. Although shale gas shows tremendous potential, there are great exploration risks in shale gas exploration due to the complicated geological conditions in China. Therefore, the prediction of hydrocarbon sweet spots is of significant importance to shale gas exploration [8–11].

Sequence stratigraphy has been successfully applied to the exploration of clastic and carbonate reservoirs since proposed nearly four decades ago [12–18]. However, the traditional sequence stratigraphy is based on the passive continental margins, with either carbonate or clastic sedimentary rocks. The application of sequence stratigraphy to deep water deposits by traditional methods faces challenges due to the weak reflection of sea level on deep water region [19, 20]. In recent years, some studies on shale sequence stratigraphy have employed various methods of lithofacies, logs and stratigraphic elemental analysis to identify sequence boundaries and the maximum flooding surface, and ultimately build sequence stratigraphy frameworks and predict the favorable intervals [21, 22].

The large-scale exploration of shale gas in recent years provides more new data for the study of shale sedimentary environment. Shale contains a variety of elements such as silicon, calcium, aluminium, uranium, thorium, potassium, iron, manganese and so on. Predecessors have been trying to identify the source of siliceous minerals in shale. Holdaway and Clayton (1982) define the concept of excess silicon, which means excessive silicon beyond the source of normal terrigenous clasts, and proposes a quantitative calculation method for excess silicon [23]. Wedepohl (1971), Adachi *et al.* (1986) and Yamamoto (1987) tried to differentiate between hydrothermal silicon and biogenic silicon by Al-Fe-Mn ternary diagram [24–26]. These two calculation methods are combined to confirm the existence and the content of excess silicon of shale by quantitative calculation. Then the causes of excess silicon is determined and sedimentary environment is analyzed. Using U/Th ratio, in combination with Ca/(Ca+Fe) and Ti/Al ratio calculations as reference, lithology and logging data, the sequence stratigraphy of shale of the Lower Cambrian is divided and accordingly the favorable intervals is identified as well.

2 Geological setting

2.1 Tectonic and sedimentary characteristics

Xiuwu basin is located in lower Yangtze area, and in the southeast of Jianghan basin. Xiuwu Basin is composed of the Luodong syncline and Xiushui-Wuning syncline. The study area is located in the west of the Xiushui-Wuning syncline, a new exploration area covering approximately 600 km^2 (Figure 1).

The Lower Cambrian is composed of Wangyinpu and Guanyintang Formations. The Early Cambrian in Xiuwu Basin lasted for about 27 million years (541–514 million years ago) [27, 28]. During the early stage of early Cambrian, a transgression occurred in the Xiuwu Basin and adjacent areas, resulting in a deep marine shelf depositional environment characterized by quiet, low-energy and anoxic conditions [27, 29]. As a result, the entire study area was covered in a thick (100-150 m) accumulation of organic-rich marine shale [28]. During the late stage of early Cambrian, the water became shallower gradually afterwards and the environment evolved into shallow-water shelf [30, 31]. In the Middle–Late Cambrian, the Xiuwu Basin, with carbonate deposits, developed in the sedimentary environment of the Epicontinental Sea.

2.2 Stratigraphic features

The underlying strata of Wangyinpu Formation is the upper sinian Piyuancun Formation, and the lithology is gray siliceous dolomite (Figure 2A). Besides, the lithology of Wangyinpu Formation is black siliceous shale (Figure 2B). The overlying strata is Guanyintang Formation, and the lithology is dark gray siliceous shale (Figure 2C). The overlying strata of Guanyintang Formation is middle Cambrian Yangliugang Formation, and the lithology is gray microcrystalline limestone (Figure 2D). The lithology of different formation are quite different. However, the lithologic variations of the Wangyinpu Formation and the Guanyintang Formation are little due to the relatively strong lithologic homogeneity of shale.

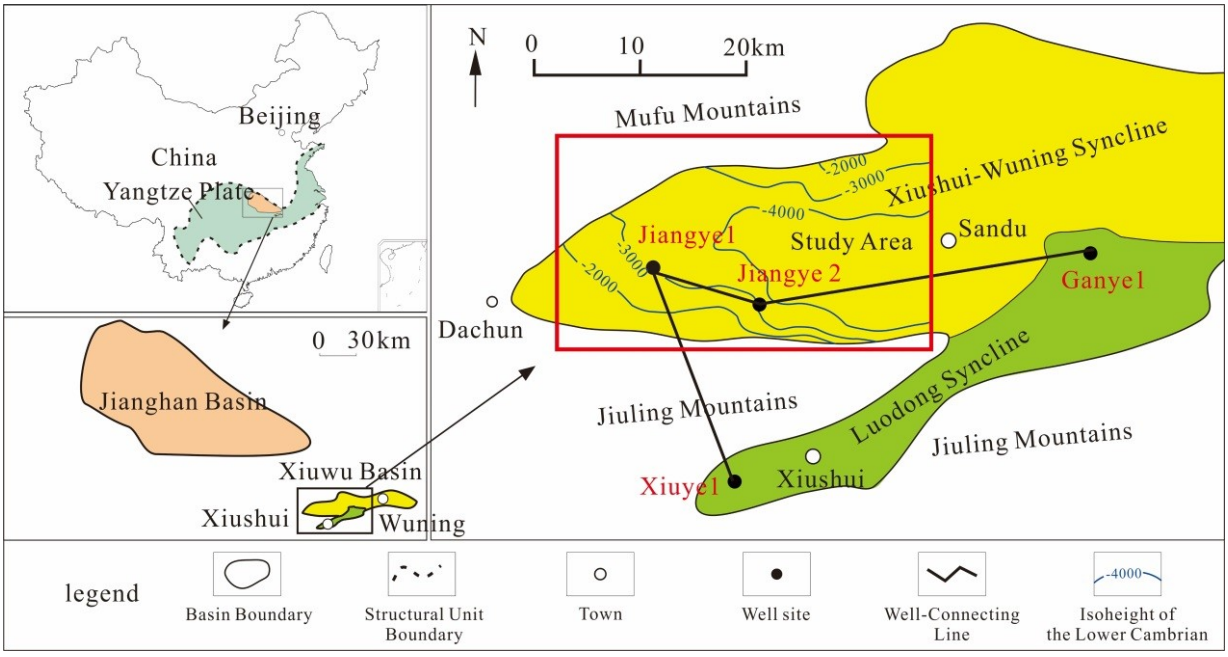

Figure 1: The geological map shows the study area with locations of wells and outcrops. Modified from references [28].

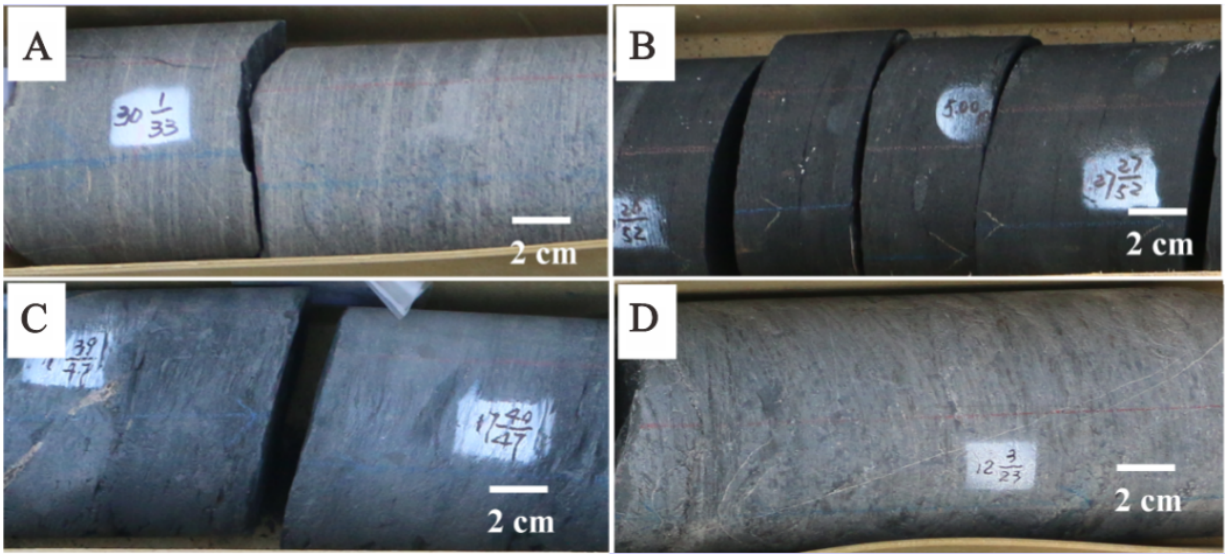

Figure 2: Core photos of Well Jiangye-1. A: Upper Sinian Piyuancun Formation 2675m, gray siliceous dolomite; B: Lower Cambrian Wangyinpu Formation 2638m, dark siliceous shale; C: Lower Cambrian Guanyintang Formation 2546m, dark gray siliceous shale; D: Middle Cambrian Yangliugang Formation 2511m, gray microcrystalline limestone. See Figure 1 for the location of the well site.

3 Samples, experiments and data source

Well Jiangye-1 located in Xiuwu Basin shale gas blocks in the Yangtze Region of Yangtze plate, is a key exploration drilling in the Lower Cambrian wells (Figure 1). Sixty five core samples were collected from Wangyinpu and Guanyintang Formation of Well Jiangye-1 every 1 to 2m. For these samples TOC content was measured by using the model for the total organic carbon analyser of OG-2000V to samples, the mineral composition of test samples was performed using ZJ207 Bruker D8 advance X-ray diffraction, the total and effective porosity were tested using PoroPDP-200 porosity measuring instrument, and the gas content was tested by YSQ-IV gas shale gas analyser. Eighty four debris samples were collected from Wangyinpu Formation and Guanyintang Formation of Well Jiangye-1 every1 to 2m. For

these samples, analysis for X-ray fluorescence spectrometry was performed using Axios-MAX model (X-Ray Fluorescence) instrument for the analysis of Al, Fe and Mn elements on the sample. All the experiments were conducted in Institute of The Unconventional Oil and Gas Resources Experimental Centre in sinopec east China branch. And this institute which is professionally accredited is professional in samples preparation and accurate in results. The logging data (GR, U, Th, CNL, AC, and DEN) and the elemental logging data (Si, Al) of Well Jiangye-1 provided by Schlumberger were collected as well. And these data were taken every 0.125m.

4 Results

4.1 Calculation of excess silicon and analysis of its cause

In order to analyse the sedimentary environment of Early Cambrian, the concept and the application of excess silicon have been introduced in the study. The source of siliceous minerals can be divided into terrestrial clastic origin, biogenic and hydrothermal origin. The excess silicon (excess siliceous mineral content) (Si_{ex}) refers to the siliceous minerals except the silicon from terrestrial clastic origin. The excess silicon content can be calculated by the following equation (Equation 1).

$$Si_{ex} = Si_s - \left[(Si/Al)_{bg} \times Al_s\right] \quad (1)$$

In the equation, Si_s is the silicous content of the samples, and Al_s stands for the aluminous content of the samples. The value of $(Si/Al)_{bg}$ is 3.11, which is the average for shale [23].

Equation 1 is used to calculate the excess silicon content of the Lower Cambrian in Well Jiangye-1. As shown in Figure 3, there are excess silicon in most of the Wangyinpu Formation and the half of the Guanyintang Formation. Specifically, the Wangyinpu Formation contains intervals with up to 40%–50% excess silicon, while intervals in the Guanyintang Formation contain relatively lower excess silicon (0%–20 %).

Excess silicon in clastic sediment can be either hydrocarbon or biogenic in origin. To differentiate between both, Wedepohl (1971), Adachi *et al.* (1986) and Yamamoto (1987) proposed the Al-Fe-Mn ternary diagram method [24–26]. The relative contents of Al, Fe and Mn were put on the ternary diagram (Figure 4). If all the points were in I area of Figure 4, it would be biological genesis. While if all the points were in II area of Figure 4, it would be hydrothermal genesis. In addition, if the points fell in between I area and II area, it would be a mixture of biological and hydrothermal genesis. In this paper, the experimental data of elements Al, Fe and Mn of intervals of the Lower Cambrian with excess silicon in Well Jiangye-1 are put in the ternary diagram. The percent normalized data of Al, Fe and Mn were all in the region of hydrothermal genesis, as shown in Figure 4, which indicates that excess silicon is of hydrothermal genesis. In the early Cambrian period, the tectonic movement at the junction of the Yangtze plate and the Cathaysia plate was relatively active, and the sea water entered the deep crustthrough the fault at the subduction boundary. Subsequently the sea water was heated, and transformed into the hydrothermal fluid. And then it returned to the ocean, in the form of submarine fountain, with siliceous minerals and other nutrient elements (nitrogen, phosphorus, potassium and so on) from the deep crust which are conducive to biological reproduction. On one hand, siliceous minerals were transformed to hydrothermal silicon in shale. On the other hand, nitrogen, phosphorus, potassium and other nutrient elements brought by upwelling were carried to the surface of the sea, which promoted the improvement of biological productivity and was conducive to the formation of organic matter in shale. Thus, the vertical siliceous source of the shale of the Lower Cambrian Wangyinpu and Guanyintang Formation in Well Jiangye-1 is accurately made, as shown on the right side of Figure 3. Most of the intervals of Wangyinpu Formation had hydrothermal silicon. More than half of the intervals contain 20%-30% hydrothermal silicon, and some of the intervals contain 30%-40%, even up to 40%-50%. While the content of hydrothermal silicon in Guanyintang Formation dropped significantly. The content of hydrothermal silicon is 10%-20% in the lower section of Guanyintang Formation, while less in the upper section of Guanyintang Formation. And the most of the silicon in the upper section of Guanyintang Formation are terrestrial clastic silicon.

The content of excess silicon can reflect the intensity of hydrothermal activity [41]. As shown in Figure 3, hydrothermal activity was widespread in the Early Cambrian in the Lower Yangtze area, and the hydrothermal activity in the Wangyinpu Formation is stronger than that in the Guanyintang Formation. Hydrothermal fluids can transport materials from deep crust to seawater. Due to the relatively strong homogeneity of shale and the mixing of new materials from the deep crust, it is difficult to identify the sequence interface of the deep water sedimentary environment under the hydrothermal influence. According to the earlier work, U/Th ratio is thought to be an indicator of the depositional environment: A high U/Th ratio is supposed

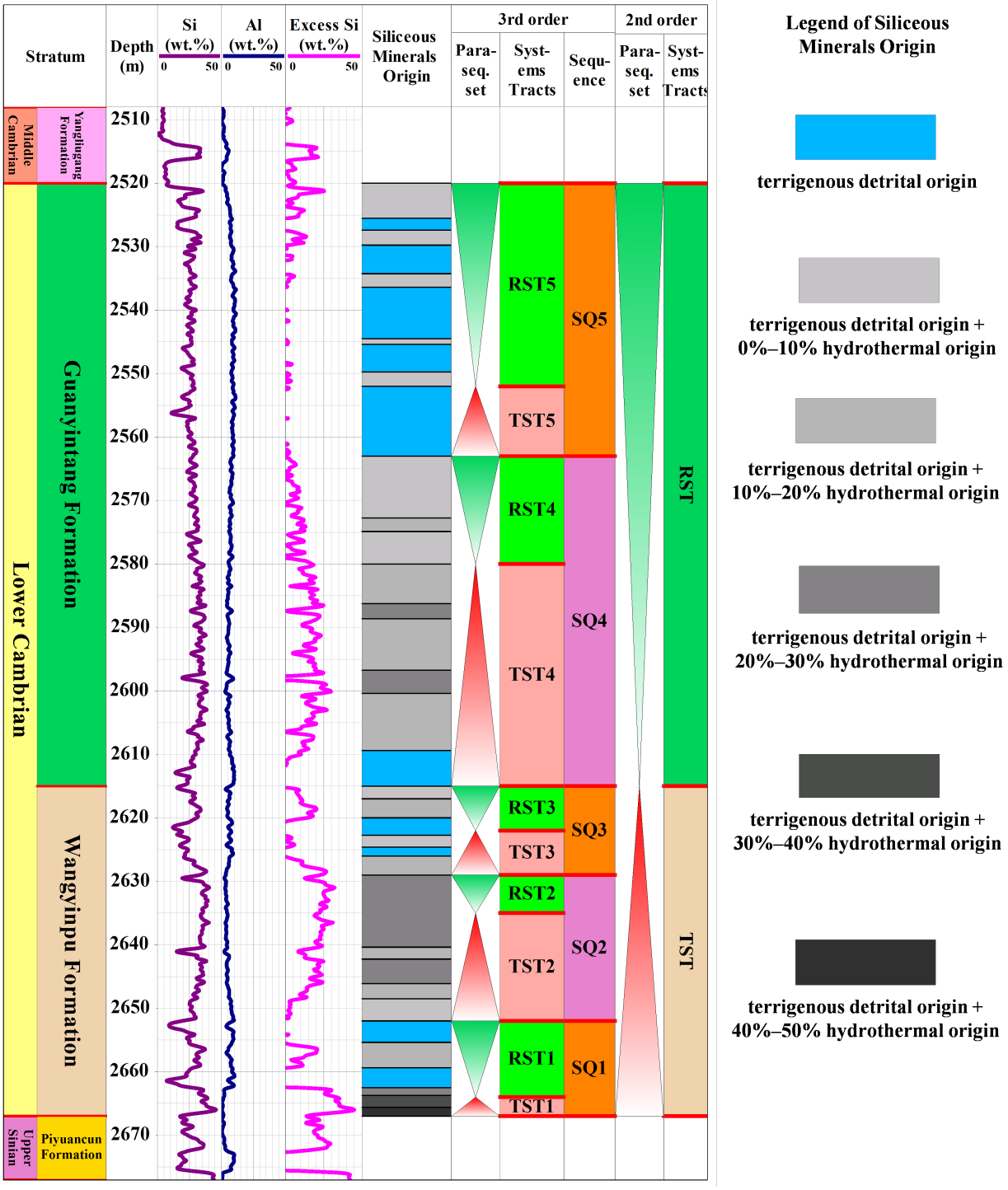

Figure 3: Analysis of content of excess silicon of the Lower Cambrian Wangyinpu and Guanyintang Formation in Well Jiangye-1 in Yangtze Region. Check Figure 1 for the well location.

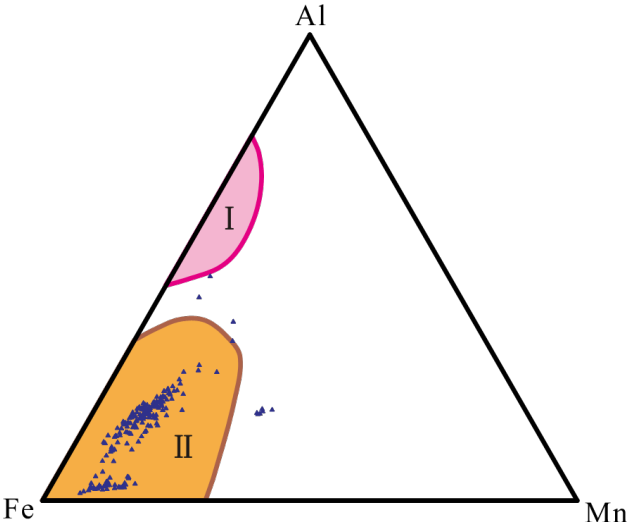

Figure 4: Al-Fe-Mn ternary diagram for analysis on sources of excess silicon of the Lower Cambrian Wangyinpu and Guanyintang Formation, showing that it is of hydrothermally genesis. The base map is from references [24–26]. See Figure 1 for the well location. I: bio-origin, II: hydrothermal origin.

to be related to a reducing environment while low U/Th ratio relates to an oxidizing environment [48–52]. Therefore, this paper mainly used the U/Th ratio and the changes of lithology as well as logging curves to divide the shale deposition sequence of deep water under the hydrothermal influence, identify favorable intervals and provide technical supports for shale gas exploration and development.

4.2 Sequence stratigraphy

4.2.1 Identification of second-order sequence boundary

It is difficult to identify the unconformity surface and ascertain the sequence boundary only by seismic reflections due to the relatively homogeneous property of the shale reservoir. Previous studies suggest that well-log data, geochemical parameters, lithofacies are of key significance for determining shale sequence boundaries [21, 53–55]. In this study, sequence boundaries are determined by a combination of redox indicator (U/Th ratio), well logs (Natural gamma ray, Uranium, Compensated neutron logging, Acoustic, Density), lithofacies.

Two sequence boundaries, SB1 (Wangyinpu Formation) and SB2 (Guantintang Formation) have been interpreted (Figure 5). SB1, the boundary between Ediacaran and Cambrian, presents unconformity between the Ediacaran Piyuancun Formation and the Cambrian Wangyinpu Formation (Figure 2A, 2B). SB1 corresponds with the argument of the previous researchers that a large-scale regression occurred during the end of the Late Ediacaran Piyuancun period and large-scale transgression began during the Early Cambrian Wangyinpu period in the Middle Yangtze area [56–59], SB1 is supposed to be a transgressive surface of erosion as Slatt and Rodriguez (2012) described [53].

Because of the regression during the end of the Late Ediacaran Piyuancun period and transgression during the Early Cambrian Wangyinpu period, light gray siliceous dolomite deposited in the Late Piyuancun period, representing a shallow water environment (Figure 2A), while black shale deposited in the Early Cambrian Wangyinpu period, representing a deep water environment (Figure 2B). This variation in lithofacies also exhibits a sharp change with respect to the well logs: SB1 was identified at a sudden change in the GR, U, CNL, AC and DEN values (Figure 5). The values of GR, U and AC increased, while the values of CNL and DEN decreased. Since in SB1 (2667m), U/Th ratio changes from low value to high value. Based on the U/Th ratio, the SB1 is a transitional surface under ancient redox conditions from increasing oxidizing conditions to increasing reduction conditions (Figure 5).

SB2 is the boundary between the Guanyintang and Yangliugang Formations, which is manifested as a lithofacies transformation interface with an underlying clastic depositional system and an overlying carbonate depositional system (Figure 2C). The variation in lithofacies also exhibits sharp changes in well logs: SB2 is identified as sudden changes in the GR, U, CNL, AC, and DEN values (Figure 5). The values of GR, U and AC decreased, while the values of CNL and DEN increased. Furthermore, changes in the U/Th ratio can be observed as well. It is obvious SB2 is an ancient redox condition transition surface with underlying increasing oxidizing conditions and overlying increasing reduction conditions based on the U/Th ratio (Figure 5).

4.2.2 Second-Order Sequences of the Lower Cambrian

According to Ogg (2004) and Gradstein *et al.*, (2004), TST of second-order sequence stratigraphy lasted 10 million years (541Ma–521Ma) while the RST lasted 7Ma (521Ma–514Ma) [60, 61]. Therefore, the Lower Cambrian is a second-order sequence. In this paper, the T-R sequence stratigraphic model was used, *i.e.*, the Transgressive Systems Tract (TST) and Regressive Systems Tract (RST) [55]. The sequence boundary is the Maximum Regressive Surface, and the systems tract interface is the Maximum Flooding Surface (MFS). RST includes highstand systems tract (HST)

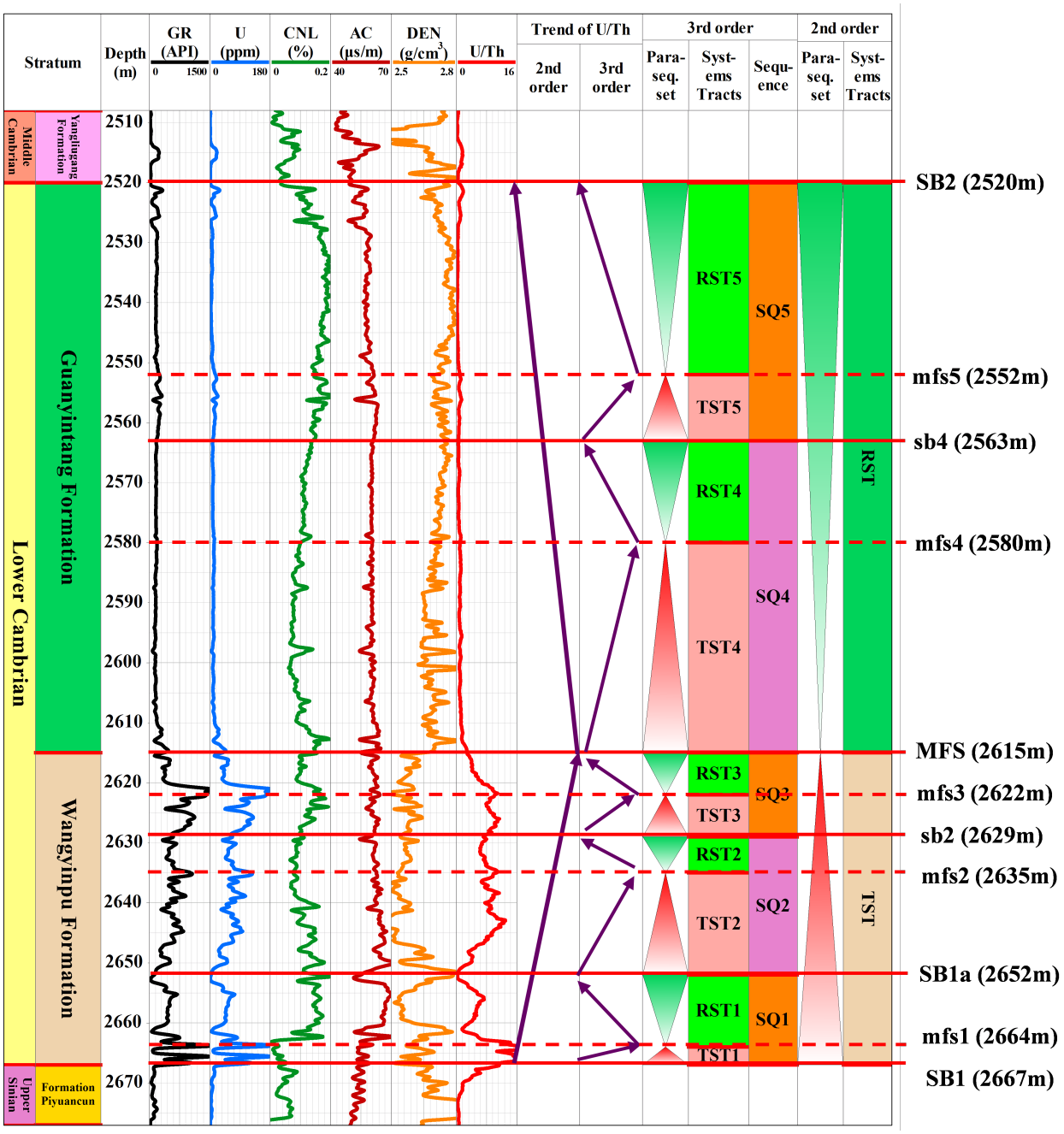

Figure 5: Division of 2nd and 3rd sequence of the Wangyinpu Formation and Guanyintang Formation of the Lower Cambrian in Well Jiangye-1 and changes in lithology vertically. See Figure 1 for the well location. SQ = Sequence; TST = Transgressive systems tract; RST = Regressive systems tract; MFS (mfs)= Maximum flooding surface; SB(sb)= Sequence Boundary; GR = Natural gamma ray; U = Uranium; CNL = Compensated neutron logging; AC = Acoustic; DEN = Density.

and lowstand systems tract (LST) according to the Vail's sequence theory [12]. Due to the lack of identification sign of the HST/LST interface and the scarcity of the LST in shelf facies, the boundary between HST and LST is difficult to distinguish. The boundary between TST and RST is interpreted as an MFS on the top of a condensed section which can be identified by the well logs, lithofacies and formation elemental features.

The Well Jiangye-1 is supposed to be an MFS at the depth of 2615 m, since the GR, U, CNL, AC, and DEN values changed suddenly, indicating a jump of lithology, porosity and gas content (Figure 5). The values of GR, U and AC decreased, while the values of CNL and DEN increased. The lithofacies from the lower section of MFS black shale is transformed into the upper dark gray siliceous shale (Figure 2). The U/Th ratio decreased suddenly from 1.25–11 to 0–1.25, indicating the sedimentary environment changed from reduction to oxygen-depleted and oxidation (Figure 5). The MFS of this second-order sequence is also the boundary between Wangyinpu and Guanyintang Formations. Therefore, TST ranges from SB1 (2667 m) to MFS (2615 m), and RST varies from MFS (2615 m) to SB2 (2520 m).

4.2.3 Third-Order Sequences of the Lower Cambrian

Lithologic differences could be observed and used to divide the TST and RST of the Lower Cambrian. Due to the strong homogeneity of the shale under hydrothermal influence and small lithologic variations, the identification of third-order sequences is extremely difficult to do using lithologic variations alone. In this study, elemental capture spectroscopy (ECS) could be applied well in the identification of third-order sequences. The MFS of third-order sequence is identified mainly according to U/Th indicator taken as references. The third-order sequences could be then subdivided into five third-order sequences (Figure 5), which sequentially are SQ1-SQ5 all consisting of TSTs and RSTs from bottom to top. Three of them are identified in the Wangyinpu Formation while the other two are in the Guanyintang Formation. Among the five third-order sequences, the TOC content, porosity, brittle mineral content and total gas content also display obvious differences with each other.

(a) SQ1 (2667–2652 m)

From 2667 m to 2664 m, the U/Th ratio increases rapidly above SB1 and then gently decreases from 2664 m to 2652 m (Figure 5). GR, U, CNL, AC and DEN present significant changes at 2652 m (Figure 5). Accordingly, the depth of 2652 m is considered to be the sequence boundary (SB1a) of the third-order sequence. At the depth of 2664 m, SQ1, the U/Th ratio reaches the maximum value (Figure 5). Thus, the depth of 2664 m is supposed to be the maximum flooding surface (mfs1) of the SQ1; the TST1 ranges from 2667 m to2664 m, and the RST1 varies from 2664 m to 2652 m (Figure 5).

(b) SQ2 (2652–2629 m)

From 2652 m to 2635 m, the U/Th ratio increases gradually above SB1a and then decreases rapidly from 2635 m to 2629 m (Figure 5). The depth of 2629 m is supposed to be the sequence boundary (sb 2) of the third-order sequence where GR, U, CNL, AC, and DEN showed obvious changes (Figure 5). At the depth of 2635 m of SQ2, the U/Th ratio reaches the highest (Figure 5). Accordingly, 2635 m is intended to be the maximum flooding surface (mfs2) of SQ2, which is also the boundary that divides the SQ2 into TST2 and RST2 (Figure 5).

(c) SQ3 (2629–2615 m)

From 2629 m to 2622 m, the U/Th ratio increases rapidly above sb2 and then reaches a high level. From 2622 m to 2615 m, the U/Th ratio decreases rapidly (Figure 5). Logging curves significantly change at 2615 m, which is also the boundary between Wangyinpu Formation and Guanyintang Formation. At the depth of 2622 m in SQ3, the U/Th ratio presents a high value (Figure 5). Therefore, the depth of 2622 m is the maximum flooding surface (mfs3) of the SQ3, which divides the SQ3 into TST3 and RST3. Specifically, the strata with the depth range of 2629–2622 m is the TST3, and with depth range of 2622 m to 2615 m is the RST3 (Figure 5).

(d) SQ4 (2615 –2563 m)

From 2615 m to 2580 m, the U/Th ratio is at consistently low value above MFS and then increases slowly. From 2580 m to 2563 m, the U/Th ratio decreases gradually (Figure 5). The depth of 2563 m is the sequence boundary (sb4) of the third-order sequence where GR, U, CNL, AC, and DEN all show distinct change (Figure 5). At the depth of 2580 m in SQ4, the U/Th ratio is at a higher value (Figure 5). Therefore, the depth of 2580 m is the maximum flooding surface

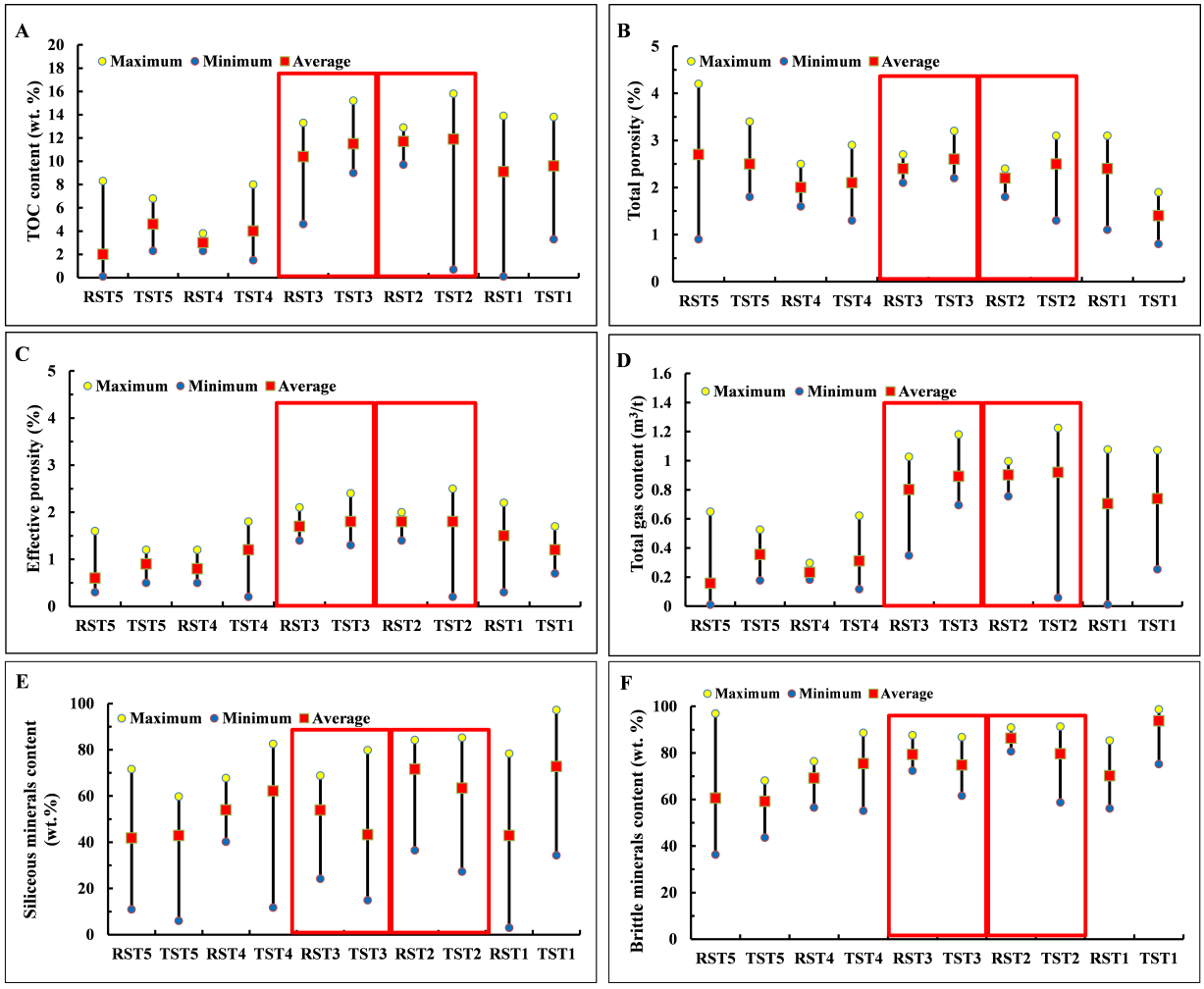

Figure 6: Variations in the TOC content, total porosity, effective porosity, total gas content, siliceous mineral content and brittle mineral content of each systems tract in the Lower Cambrian of Well Jiangye-1. See Figure 1 for the well location.

(mfs4) of the SQ4. The depth range of 2615–2580 m is the TST4, and the depth from 2580 m to 2563 m is the RST4 (Figure 5).

(e) SQ5 (2563–2520 m)

From 2563 m to 2552 m, the U/Th ratio increases rapidly and then decreases slowly to a low value from 2552 m to 2520 m (Figure 5). The depth of 2520 m is also the upper boundary of Guanyintang Formation. At the depth of 2552 m in SQ5, the U/Th ratio shows a relatively higher value (Figure 5). Therefore, the depth of 2552 m is the maximum flooding surface (mfs5) dividing SQ5 into TST5 and RST5 tow parts, specifically. The strata with depth of 2563–2552 m is TST5, and that of 2552–2520 m is RST5 (Figure 5).

4.3 TOC, porosity, mineralogy and total gas content within sequence stratigraphy

In the second-order sequence (Wangyinpu Formation and Guanyintang Formation), the TOC content, total porosity, effective porosity, siliceous mineral content, brittle mineral content and total gas content all display variations from SQ1 to SQ5 (Figure 6A–6F).

Generally, it can be concluded that the TOC content is higher than 8% in SQ1, SQ2 and SQ3 and then sharply decreases to 2%–4% in SQ4 and SQ5. Besides, in each third-order sequence, the TOC content of TST is evidently higher than RST. Specifically, in Wangyinpu Formation, the TOC content of SQ2 and SQ3 is relatively higher than SQ1 (Figure 6A).

Apart from TST1, the average total porosity of the system tracts of the five sequences is approximately 2%–3%. Among the five sequences, the total porosity distribution

of SQ5 shows the highest heterogeneity (Figure 6B). However, the distribution trend of effective porosity is obviously distinct from total porosity. In these sequences, the effective porosity of SQ1 is 1%–1.5%, and that of SQ2 and SQ3 increases to 1.5%–2%, and it suddenly decreases to below 1% in most sections of SQ4 and SQ5 (Figure 6C). The effective porosity of SQ2 is the highest among the five sequences, which increases from 1% at the bottom to 2.2% at the top of TST2 and then decreases to 1.8% in RST2. The trend of effective porosity of SQ3 is similar to SQ2, increasing from 1.9% to 2.4% in TST3 and then decreasing to 1.6% in RST3 (Figure 6C).

The total gas content shows drastic changes in this second-order sequence. The average value decreases from 0.8 m^3/ton in Wangyinpu Formation to 0.2 m^3/ton in Guanyintang Formation. The average total gas content of SQ2 is 0.911m^3/ton and that of SQ3 is 0.847 m^3/ton. Both are higher than that of SQ1 (0.722 m^3/ton). Furthermore, the average total gas content of TST2 (0.92 m^3/ton) is slightly higher than that of RST2 (0.902 m^3/ton), and TST3 (0.892 m^3/ton) is also higher than RST3 (0.802 m^3/ton) (Figure 6D).

It can be also concluded that mineral composition shows obvious variations among different sequences. In SQ1–SQ3, the siliceous mineral content changes considerably from 40% to 80%. In SQ4–SQ5, the siliceous mineral content generally decreases from 62.2% to 41.8% (Figure 6E). Compared with the siliceous mineral content, the brittle mineral content shows a regular change. In SQ1–SQ3, the brittle mineral content is approximately 80%, while gradually decreases to 60% in SQ4–SQ5, corresponding to the increase of the clay mineral content (Figure 6F).

5 Discussion

Combining sequence with the results of analysis of excessive silicon content, as shown in Figure 3. Because excessive silicon content reflects the hydrothermal activity, the Figure 3 shows that excess silicon content changes a lot during the sedimentation of SQ1. It shows that hydrothermal activities are strong sometimes while weak sometimes. Hydrothermal activities during depositional process of SQ2 and SQ3 are relatively active, and the excessive silicon content are both above 20%-30%. But when depositional process of SQ4, hydrothermal activities weaken greatly and hydrothermal silicon content is 10%-20%. There are nearly no hydrothermal activities during the depositional process of SQ5, and most are terrigenous clastic silicon. Previous researches shows that the hydrothermal activities play important role for organic matter [37–44]. On the one hand, hydrothermal activities can carry nutritions which are advantageous to the growth of plankton and is beneficial to the improvement of the biological productivity. On the other hand, because the hydrotherm from the deep crust, it is a lack of oxygen to promote an anaerobic environment at the bottom of sea water. As a result, the organic matter can be preserved. To sum up, the hydrothermal activities can not only bring rich hydrothermal genesic siliceous minerals, but also promote the enrichment of organic matter.

Because SQ2 and SQ3 are in the period of transgression under the second-order deposition sequence, the sea level rises, and deep water is conducive to the formation of reducing environment. In addition, hydrothermal activity is relatively developed at this time, which is beneficial to the improvement of biological productivity and the preservation of organic matter, and thus the accumulation of organic matter. Shale gas is mainly stored in organic matter pores, and organic matter pores provide natural gas main flowing channels [62–66]. The content of TOC in SQ4 and SQ5 is much lower than that of SQ2 and SQ3, and the gas content is low. SQ2 and SQ3 possess the highest TOC content, effective porosity, total gas content and brittle mineral content among these sequences. SQ2 and SQ3 are the most favorable intervals for the vertical accumulation of shale gas in the lower Cambrian in Xiuwu Basin. Due to the relatively strong homogeneity of shale, other new drilling in this block can be divided into the sequence by the same method. And the favorable intervals can be selected directly without organic geochemical experiments, mineral composition analysis experiments and gas content analysis, which can save a lot of costs and time.

6 Conclusions

In this paper, the marine shale of the Lower Cambrian Wangyinpu and Guanyintang Formation in Chinese Southern the Lower Yangtze Region is taken as the research intervals, Well Jiangye-1 in Xiuwu Basin as the research object, using data of elemental analysis, logging, lithofacies, mineral composition, effective porosity, TOC content, gas content and so on, analyzing sequence stratigraphy of the Early Cambrian shale in the Lower Yangtze Region, drawing the following conclusions.

(1) In the Lower Cambrian shale in Yangtze Region, there are still a lot of siliceous minerals of hydrothermal origin in most intervals of the wells except for the origin of normal terrigenous clasts. During the

deposition of SQ2 and SQ3, hydrothermal activity was more active, and their excess silicon content was generally above 20%-30%.

(2) When it comes into shale of hydrothermal origin, in this paper the sequence stratigraphic characteristics are analyzed by stratigraphic elements U/Th ratio, lithology and logging data. The strata of the Lower Cambrian can be defined as a second-order sequence, composed of a transgressive system tract (TST) and a regressive system tract (RST). The strata can be further subdivided into five third-order sequences with different mineral compositions (SQ1–SQ5).

(3) Hydrothermal activity is conducive to the enrichment of organic matter and can bring more siliceous minerals. At the same time, rising sea level is beneficial to the formation of anoxic environment at the bottom of water. Compared with the other third-order sequences, SQ2 and SQ3 have higher TOC content, brittle mineral content, effective porosity and gas content due to the active hydrothermal activity and rising sea level. Therefore SQ2 and SQ3 are considered to be the most favourable pay zones within the sequence stratigraphy framework in the Xiuwu Basin.

Acknowledgement: This study was supported by the National Science and Technology Major Project (No. 2017ZX05035-002), the Science Foundation of the Ministry of Land and Resources of China (No.12120114046701), the National Natural Science Foundation of China (No. 41472112 and No. 41728004) and open fund from Sinopec Key Laboratory of Shale Oil/Gas Exploration and Production Technology. All of the critical comments and constructive suggestions from anonymous reviewers and the editors are appreciated sincerely.

References

[1] Curtis, J.B., Fractured shale-gas systems. AAPG Bull., 2002, 86 (11), 1921-1938

[2] Montgomery, S.L., Jarvie, D.M., Bowker, K.A., Pollastro, R.M., Mississippian barnett shale, fort Worth Basin, north-central Texas: gas-shale play with multitrillion cubic foot potential. AAPG Bull., 2005, 89 (2), 155-175

[3] Warlick D., Gas shale and CBM development in North America. Oil & Gas Financial Journal, 2006, 3(11), 1-5

[4] Dong, D., Wang, Y., Li, X., Zou, C., Guan, Q., Zhang, C., Huang, J., Wang, S., Wang, H., Liu, H., Bai, W., Liang, F., Lin, W., Zhao, Q., Liu, D., Qiu, Z., Breakthrough and prospect of shale gas exploration and development in China. Natural Gas Industry, 2016, 36 (1), 19-32 (in Chinese with English abstract)

[5] Guo, T., Key geological issues and main controls on accumulation and enrichment of Chinese shale gas. Petrol. Explor. Dev., 2016, 43 (3), 317-326 (in Chinese with English abstract)

[6] Guo, X., Hu, D., Wei, Z., Li, Y., Wei, X., Discovery and exploration of Fuling shale gas field. China Petroleum Exploration, 2016, 21(3), 24-37 (in Chinese with English abstract)

[7] Wei, X., Zhao, Z., Wang, Q., Liu, Z., Zhou, M., Zhang, H., Comprehensive Evaluation of Geological Conditions of the Shale Gas in Upper Ordovician Wufeng Formation-Lower Silurian Longmaxi Formation in Dingshan Area, Qijiang, Southeastern Sichuan. Geological Review, 2017, 63(1), 153-164 (in Chinese with English abstract)

[8] Chen, L., Jiang, Z., Liu, K., Wang, P., Ji, W., Gao, F., Hu, T., Zhang, B., Huang, H., Effect of lithofacies on gas storage capacity of marine and continental shales in the Sichuan Basin, China. J. Nat. Gas. Sci. Eng., 2016, 36, 773-785

[9] Chen, L., Jiang, Z., Liu, K., Tan, J., Gao, F., Wang, P., Pore structure characterization for organic-rich Lower Silurian shale in the Upper Yangtze Platform, South China: A possible mechanism for pore development. J. Nat. Gas. Sci. Eng., 2017, 46, 1-15

[10] Zhu, H., Deng, J., Jin, X., Hydraulic Fracture Initiation and Propagation from Wellbore with Oriented Perforation. Rock Mech. Rock Eng., 2015, 48(2), 585-601

[11] Zhu, H., Jin, X., Guo, J., Coupled flow, stress and damage modelling of interactions between hydraulic fractures and natural fractures in shale gas reservoirs. Int. J. Oil Gas Coal T., 2016, 13(4), 359-390

[12] Vail, P.R., Mitchum Jr., R.M., Todd, R.G., Seismic stratigraphy and global changes in sea level. AAPG Memoir, 1977, 26, 49-62

[13] Van Wagoner, J.C., Mitchum, R.M., Campion, K.M., Rahmanian, V.D., Siliciclastic sequence stratigraphy in well logs, cores, and outcrop: concepts for high resolution correlation of time and facies. AAPG Methods in Exploration Series, 1990, 7, 1-63

[14] Weimer, P., Varnai, P.P., Budhijanto, F.M., Sequence stratigraphy of Pliocene and Pleistocene turbidite systems, northern Green Canyon and Ewing Bank (offshore Louisiana), northern Gulf of Mexico, AAPG Bull., 1998, 82 (5), 918-960

[15] Catuneanu, O., Sequence stratigraphy of clastic systems: concepts, merits, and pitfalls. J. Afr. Earth Sci., 2002, 35, 1-43

[16] Lash, G., Engelder, T., Thickness trends and sequence stratigraphy of the middle Devonian Marcellus formation, Appliachian basin: implications for Acadian foreland basin evolution. AAPG Bull., 2011, 95(1), 61-103

[17] Jiang, S., Henriksen, S., Wang, H., Lu, Y., Ren, J., Cai, D., Feng, Y., Weimer, P., Sequence-stratigraphic architectures and sandbody distribution in Cenozoic rifted lacustrine basins, east China. AAPG Bull., 2013, 97(9), 1447-1475

[18] Zhang, K., Jiang, Z., Xie, X., Gao, Z., Liu, T., Yin, L., Jia, C., Song, Y., Shan, C., Wu, Y., Wang, P., Lateral Percolation and Its Effect on Shale Gas Accumulation on the Basis of Complex Tectonic Background. Geofluids, 2018, doi: 10.1155/2018/5195469

[19] Almon, W.R., Dawson, W.C., Sutton, S.J., Ethridge, F.G., Castelblanco, B., Sequence stratigraphy, facies variation, and petrophysical properties in deep water shales, Upper Cretaceous Lewis Shale, south-central Wyoming. Gulf Coast Association of Geological Society Transactions, 2002, 52, 1041-1053

[20] Hemmesch, N.T., Harris, N.B.C., Minch, A., Selby, D., A sequence-stratigraphic framework for the Upper Devonian Woodford Shale, Permian Basin, west Texas. AAPG Bull., 2014, 98(1), 23-47

[21] Abouelresh, M.O., Slatt, R.M., Lithofacies and sequence stratigraphy of the Barnett shale in the east-central Fort Worth Basin, Texas. AAPG Bull., 2012, 96(1), 1-22
[22] Chen, L., Lu, Y., Jiang, S., Li, J., Guo, T., Luo, C., Heterogeneity of the Lower Silurian Longmaxi marine shale in the southeast Sichuan Basin of China. Mar. Petrol. Geol., 2015, 65, 232-246
[23] Holdaway, H.K., Clayton, C.J., Preservation of shell microstructure in silicified brachiopods from the upper cretaceous Wilmington sands of Devon. Geol. Mag., 1982, 119, 371–382
[24] Wedepohl, K.H., Environmental influences on the chemical composition of shales and clays. Phys. Chem. Earth, 1971, 8, 307-331
[25] Adachi, M., Yamamoto, K., Sugisaki, R., Hydrothermal chert and associated siliceous rocks from the Northern Pacific: their geological significance as indication of ocean ridge activity. Sediment. Geol., 1986, 47 (1), 125-148
[26] Yamamoto, K., Geochimical characteristics and depositional environments of cherts and associated rocks in the Franciscan and Shimanto terrenes. Sediment. Geol., 1987, 52, 65-108
[27] Feng, Z., Peng, Y., Jin, Z., Lithofacies paleogeography of the Cambrian in South China. Journal of Paleogeography, 2001, 3(1), 1-14 (in Chinese with English abstract)
[28] Liu, W., Tian J., Lin X., Shi, J., Yang, C., Peng, S., Characteristics and significance of mineral compositions in Lower Cambrian black shale from Xiuwu Basin, Jiangxi, China. Journal of Chengdu University of Technology (Science & Technology Edition). 2015, 42 (1), 90-97 (in Chinese with English abstract)
[29] Yang, J., Yi, F., Hou, L., Genesis and petrogeochemistry characteristics of Lower Cambrian black shale series in northern Guizhou. Acta Mineralologica Sinica, 2004, 24(3), 286-291 (in Chinese with English abstract)
[30] Qi, X., Hu, Q., Yi, X., Zhang, S., Shale gas exploration prospect of Lower Cambrian Wangyinpu formation in Xiuwu Basin. China Mining Magazine, 2015, 24(10), 102-107 (in Chinese with English abstract)
[31] Wang, G., Ju, Y., Han, K., Early Paleozoic shale properties and gas potential evaluation in Xiuwu Basin, western Lower Yangtze Platform. J. Nat. Gas Sci. Eng., 2015, 22, 489-497
[32] Bostrom, K., Kraemer, T., Gratner, S., Provenance and accumulation rates of opaline silica, Al, Ti, Fe, Mn, Cu, Ni, and Co in Pacific pelagic sediments. Chem. Geol., 1973, 11(2), 123-148
[33] Murray, R.W., Buchholtz, T. B. M. R., Gerlach, D.C., Rare earth, major, and trace elements in chert form the Franciscan complex and monterey group, California: assessing REE sources to fine-grained marine sediments. Geochim. Cosmochim. Ac., 1991, 55 (7), 1875-1895
[34] Liu, J., Zheng, M., Geochemistry of hydrothermal sedimentary silicalite. Acta Geological Sichuan, 1993,13(2), 110-118 (in Chinese with English abstract)
[35] Yang, J., Wang, D., Mao, J. *et al.*, The petrochemical research method for silicalite and its application to the Jingtieshan Type iron deposits. Acta Petrologica et Mineralogical, 1999, 18(2), 108-118 (in Chinese with English abstract)
[36] Liu, J., Li, Y., Zhang, Y., Liu, S., Cai, Y., Evidences of biogenic silica of Wufeng-Longmaxi Formation shale in Jiaoshiba area and its geological significance. Journal of China University of Petroleum (Edition of Natural Science), 2017, 41 (1), 34-41 (in Chinese with English abstract)
[37] Sun, X., Chen, J., Liu, W., Zhang, S., Wang, D., Hydrothermal venting on the seafloor and formation of organicerich sediments: evidence from the NeoProterozoic Xiamaling Formation, North China. Geol. Rev., 2003, 49(6), 588-595 (in Chinese with English abstract)
[38] Sun, X., Chen, J., Zheng, J., Liu, W., Geochemical characteristics of organic matter-rich sedimentary strata in lower Cambrian, Tarim Basin and its origins. Acta Sedimentol. Sin. 2004, 22 (3), 548-552 (in Chinese with English abstract)
[39] Zhang, W., Yang, H., Xie, L., Yang, Y., Lake-bottom hydrothermal activities and their influences on the high-quality source rock development: a case from Chang 7 source rocks in Ordos Basin, China. Petrol. Explor. Dev., 2010, 37(4), 424-429 (in Chinese with English abstract)
[40] He, J., Duan, Y., Zhang, X., Wu, B., Xu, L., Hydrocarbon generation conditions of the shale in niutitang formation of lower Cambrian, Southern Chongqing and Northern Guizhou, China. Mar. Geol. Front., 2011, 27 (7), 34-40 (in Chinese with English abstract)
[41] Zhang, K., Jiang, Z., Yin, L., Gao, Z., Wang, P., Song, Y., Jia, C., Liu, W., Liu, T., Xie, X., Li, Y., Controlling functions of hydrothermal activity to shale gas content-taking lower Cambrian in Xiuwu Basin as an example. Mar. Pet. Geol. 2017, 85, 177-193
[42] Zhang, K., Li, Z., Jiang, S., Jiang, Z., Wen, M., Jia, C., Song, Y., Liu, W., Huang, Y., Xie, X., Liu, T., Wang, P., Shan, C., Wu, L., Comparative Analysis of the Siliceous Source and Organic Matter Enrichment M42echanism of the Upper Ordovician-Lower Silurian Shale in the Upper-Lower Yangtze Area. Minerals, 2018, 8, doi:10.3390/min8070283
[43] Zhang, K., Song, Y., Jiang, S., Jiang, Z., Jia, C., Huang, Y., Liu, X., Wen, M., Wang, X., Li, X., Wang, P., Shan, C., Liu, T., Liu, W., Xie, X., 2019. Shale gas accumulation mechanism in a syncline setting based on multiple geological factors: An example of southern Sichuan and the Xiuwu Basin in the Yangtze Region. Fuel 241 (2019), 468–476
[44] Zhang, K., Song, Y., Jiang, S., Jiang, Z., Jia, C., Huang, Y., Wen, M., Liu, W., Xie, X., Liu, T., Wang, P., Shan, C., Wu, Y., 2019. Mechanism analysis of organic matter enrichment in different sedimentary backgrounds: A case study of the Lower Cambrian and the Upper Ordovician-Lower Silurian, in Yangtze region. Mar. Petrol. Geol.99, 488–497.
[45] McKibben, M.A., Williams, A.E., Hall, G.E.M., Solubility and transport of plantinum-group elements and Au in saline hydrothermal fluids; constraints from geothermal brine data. Econ. Geol., 1990, 85 (8), 1926-1934
[46] Korzhinsky, M.A., Tkachenko, S.,I., Shmlovich, K.,I., Discovery of a pure rhenium mineral at Kudriavy volcano. Nature, 1994, 369, 51-52
[47] Halbach, M., Koschinsky, A., Halbach, P., Report on the discovery of gallionella ferruginea from an active hydrothermal field in the deep sea. Int. Ridge-Crest Res., 2001,10(1), 18-20
[48] Hatch, J.R., Leventhal, J.S., Relationship between inferred redox potential of the depositional environment and geochemistry of the Upper Pennsylvanian (Missourian) stark shale member of the Dennis Limestone, Wabaunsee County, Kansas, U.S.A.. Chem. Geol., 1992, 99 (1/3), 65-82
[49] Jones, B., Manning, D.A.C., Comparison of geochemical indices used for the interpretation of palaeoredox conditions in ancient mudstones. Chem. Geol., 1994, 111 (1/4), 111-129
[50] Kimura, H., Watanabe, Y., Ocean anoxia at the Precambrian-Cambrian boundary. Geology, 2001, 29 (11), 995-998
[51] Chen, L., Lu, Y., Jiang, S., Li, J., Guo, T., Luo, C., Xing, F., Sequence stratigraphy and its application in marine shale gas exploration: A case study of the Lower Silurian Longmaxi Formation

in the Jiaoshiba shale gas field and its adjacent area in southeast Sichuan Basin, SW China. J. Nat. Gas Sci. Eng., 2015, 27(2), 410-423

[52] Wang, G., Ju, Y., Han, K., Early Paleozoic shale properties and gas potential evaluation in Xiuwu Basin, western Lower Yangtze Platform. J. Nat. Gas Sci. Eng., 2015(22), 489-497

[53] Slatt, R.M., Rodriguez, N.D., Comparative sequence stratigraphy and organic geochemistry of gas shales: commonality or coincidence. J. Nat. Gas Sci. Eng., 2012, 8, 68-84

[54] Abdel-Fattah, M.I., Slatt, R.M., Sequence stratigraphic controls on reservoir characterization and architecture: case study of the Messinian Abu Madi Incised-Valley Fill, Egypt. Cent. Eur. J. Geosci., 2013, 5 (4), 497-507

[55] Wang, T., Yang, K., Xiong, L., Shi, H., Zhang, Q., Wei, L., He, X., Shale sequence stratigraphy of Wufeng-Longmaxi Formation in southern Sichuan and their control on reservoirs. Acta Petrolei Sinica, 2015, 36(8), 915-925(in Chinese with English abstract)

[56] Fan, D., Ye, J., Yang, R., Huang, Z., The geological events and mineralization near the boundary line of Precambrian and Cambrian in Yangtze Platform, Acta Sedimentologica Sinica. 1987, 5(3), 81-95 (in Chinese with English abstract)

[57] Li, Z., Lu, Y., Wang, J., Duan, T., Gao, Y., Sedimentary characteristics and lithofacies palaeogeography of the Late Sinian and Early Cambrian in middle Yangtze region. Journal Of Palaeogeography, 2004, 6(2), 151-161 (in Chinese with English abstract)

[58] Wang, Y., Chen, J., Hu, L., Zhu, Y., Sedimentary environment control on shale gas reservoir: A case study of Lower Cambrian Qiongzhusi Formation in the Middle Lower Yangtze area. Journal of China Coal Society, 2013, 38(5), 845-850 (in Chinese with English abstract)

[59] Liu, Q., Tao, L., Zhu, H., Macroscale Mechanical and Microscale Structure Changes in Chinese Wufeng Shale with Supercritical Carbon Dioxide Fracturing. SPE J., 2017, 23(3), 691-703

[60] Ogg, J.G., Status of divisions of the International Geologic Time Scale. Lethaia, 2004, 37(2), 183-199

[61] Gradstein, F.M., Ogg, J.G., Smith, A.G., Bleeker, W., Lourens, L.J., A new Geologic Time Scale, with special reference to Precambrian and Neogene. Episodes, 2004, 27 (2), 83-100

[62] Tang, X., Jiang, Z., Li, Z., Gao, Z., Bai, Y., Zhao, S., Feng, J., The effect of the variation in material composition on the heterogeneous pore structure of highmaturity shale of the Silurian Longmaxi formation in the Southeastern Sichuan Basin, China. J. Nat. Gas. Sci. Eng., 2015, 23, 464-473

[63] Tang, X., Jiang, Z., Jiang, S., Wang, P., Xiang, C., Effect of organic matter and maturity on pore size distribution and gas storage capacity in high-mature to post-mature shales. Energy & Fuels, 2016, 30 (11), 8985-8996

[64] Tang, X., Jiang, Z., Jiang, S., Cheng, L., Zhang, Y., Characteristics and origin of insitu gas desorption of the Cambrian Shuijingtuo Formation shale gas reservoir in the Sichuan Basin, China. Fuel, 2017, 187, 285-295

[65] Wang, P., Jiang, Z., Chen, L., Yin, L., Li, Z., Zhang, C., Tang, X., Wang, G., Pore structure characterization for the Longmaxi and Niutitang shales in the Upper Yangtze Platform, South China: evidence from focused ion beam-He ion microscopy, nano-computerized tomography and gas adsorption analysis. Mar. Petrol. Geol., 2016, 77, 1323-1337

[66] Wang, P., Jiang, Z., Ji, W., Zhang, C., Yuan, Y., Chen, L., Yin, L., Heterogeneity of intergranular, intraparticle and organic pores in Longmaxi shale in Sichuan Basin, South China: evidence from SEM digital images and fractal and multifractal geometries. Mar. Petrol. Geol., 2016, 72, 122-138